Journal of Experimental Botany
doi:10.1093/jxb/eru427
This paper is available online free of all access charges (see http://jxb.oxfordjournals.org/open_access.html for further details)

Journal of Experimental Botany
www.jxb.oxfordjournals.org

RESEARCH PAPER

Cellular inorganic carbon fluxes in *Trichodesmium*: a combined approach using measurements and modelling

Meri Eichner[1,*], Silke Thoms[1], Sven A. Kranz[2,3] and Björn Rost[1]

[1] Marine Biogeosciences, Alfred Wegener Institute, Helmholtz Centre for Polar and Marine Research, Am Handelshafen 12, 27570 Bremerhaven, Germany
[2] Department for Geosciences, Princeton University, 08540 Princeton, NJ, USA
[3] Present address: Department of Earth, Ocean and Atmospheric Sciences, Florida State University, Tallahassee, Fl, 32306, USA

* To whom correspondence should be addressed. E-mail: meri.eichner@awi.de

Received 4 June 2014; Revised 3 September 2014; Accepted 23 September 2014

Abstract

To predict effects of climate change on phytoplankton, it is crucial to understand how their mechanisms for carbon acquisition respond to environmental conditions. Aiming to shed light on the responses of extra- and intracellular inorganic C (C_i) fluxes, the cyanobacterium *Trichodesmium erythraeum* IMS101 was grown with different nitrogen sources (N_2 vs NO_3^-) and pCO_2 levels (380 vs 1400 µatm). Cellular C_i fluxes were assessed by combining membrane inlet mass spectrometry (MIMS), ^{13}C fractionation measurements, and modelling. Aside from a significant decrease in C_i affinity at elevated pCO_2 and changes in CO_2 efflux with different N sources, extracellular C_i fluxes estimated by MIMS were largely unaffected by the treatments. ^{13}C fractionation during biomass production, however, increased with pCO_2, irrespective of the N source. Strong discrepancies were observed in CO_2 leakage estimates obtained by MIMS and a ^{13}C-based approach, which further increased under elevated pCO_2. These offsets could be explained by applying a model that comprises extracellular CO_2 and HCO_3^- fluxes as well as internal C_i cycling around the carboxysome via the CO_2 uptake facilitator NDH-1_4. Assuming unidirectional, kinetic fractionation between CO_2 and HCO_3^- in the cytosol or enzymatic fractionation by NDH-1_4, both significantly improved the comparability of leakage estimates. Our results highlight the importance of internal C_i cycling for ^{13}C composition as well as cellular energy budgets of *Trichodesmium*, which ought to be considered in process studies on climate change effects.

Key words: Carbon acquisition, carbon-concentrating mechanism (CCM), CO_2, cyanobacteria, leakage, NDH, ocean acidification.

Introduction

Cyanobacteria are ancient organisms responsible for oxygenation of the atmosphere during times when CO_2 concentrations were about two orders of magnitude higher than today (cf. Buick, 1992; Kasting and Siefert, 2002). Possibly due to their origin at that time, the CO_2-fixing enzyme RubisCO of cyanobacteria has one of the lowest affinities among all autotrophic organisms (Badger *et al.*, 1998; Tortell, 2000). Consequently, cyanobacteria are dependent on high activities of carbon-concentrating mechanisms (CCM) for increasing the CO_2 concentration in the vicinity of RubisCO. Currently, due to ongoing anthropogenic CO_2 combustion, the availability and speciation of inorganic C (C_i) in seawater is changing

Abbreviations: a_{carb}, fractional contribution of HCO_3^- to total C_i uptake into the carboxysome; a_{cyt}, fractional contribution of HCO_3^- to total C_i uptake into the cytosol; CA, carbonic anhydrase; CCM, carbon-concentrating mechanism; chl *a*, chlorophyll *a*; C_i, inorganic carbon; DIC, dissolved inorganic carbon; $K_{1/2}$, half-saturation concentration; L_{13C}, leakage calculated from ^{13}C fractionation; L_{carb}, modelled leakage from the carboxysome; L_{cyt}, modelled leakage over the plasma membrane; L_{MIMS}, leakage estimated by MIMS; MIMS, membrane inlet mass spectrometry; POC, particulate organic carbon; PQ, photosynthetic quotient; V_{max}, maximal rate; ε_{cyt}, ^{13}C fractionation in the cytosol; ε_{db}, ^{13}C equilibrium fractionation in the external medium, ε_p, total ^{13}C fractionation during POC formation; ε_{Rub}, ^{13}C fractionation by RubisCO.

at a rapid pace (IPCC, 2007). In view of this ocean acidification (Caldeira and Wickett, 2003), a number of studies in recent years have focused on the mechanisms of C acquisition and CO_2 responses of different groups of phytoplankton (e.g. Rost *et al.*, 2008). Among these studies, the abundant N_2-fixing cyanobacterium *Trichodesmium* stands out by showing an exceptionally high stimulation of biomass production and N_2 fixation in response to elevated pCO_2 (e.g. Hutchins *et al.*, 2007; Levitan *et al.*, 2007; Kranz *et al.*, 2009). Further studies on the underlying reasons for these CO_2 effects show a decrease in C_i affinity at high pCO_2 (Kranz *et al.*, 2009; Kranz *et al.*, 2010). Given the high energy demand of the CCM in cyanobacteria, a reallocation of energy between C_i acquisition and N_2 fixation was suggested to stimulate production at high pCO_2 (Kranz *et al.*, 2010).

Cellular C_i affinities of *Trichodesmium* are determined by the interplay of several transporters and structural adaptations composing the CCM. In order to understand pCO_2 responses of the CCM as well as potential changes in energy demand, it is necessary to distinguish between these different components. While CO_2 can diffuse through the cell membrane without energy investments, the low equilibrium concentrations, slow interconversion with HCO_3^- (Zeebe and Wolf-Gladrow, 2007), and its tendency to leak out of the cell compromise the use of CO_2 as the predominant C_i source. Therefore, cyanobacteria have evolved energy-dependent transporters for taking up HCO_3^-, which can be accumulated in the cell more efficiently (Badger *et al.*, 2006). *Trichodesmium* has been found to cover ~90% of its C demand using HCO_3^- (Kranz *et al.*, 2009; Kranz *et al.*, 2010). Uptake of HCO_3^- in this species is catalysed by the Na^+-dependent transporter BicA, which is fuelled by Na^+/HCO_3^- symport or via an H^+/Na^+ antiport mechanism (Price *et al.*, 2008).

Cyanobacterial RubisCO is localized in distinct compartments within the cell, the so-called carboxysomes. The protein shells of these microbodies are permeable to HCO_3^- but pose a diffusion barrier for CO_2 (Dou *et al.*, 2008; Espie and Kimber, 2011), allowing significant accumulation of CO_2 in the vicinity of RubisCO. Inside the carboxysomes, transformation of HCO_3^- to CO_2 is accelerated by carbonic anhydrase (CA; reviewed by Espie and Kimber, 2011). In addition to direct HCO_3^- uptake and CO_2 diffusion, CO_2 uptake in *Trichodesmium* is facilitated by the NDH-1_4 complex, which converts CO_2 to HCO_3^- in the cytoplasm, presumably in a CA-like reaction (Price *et al.*, 2002). The protein complex is thought to be located on the thylakoid membrane and form part of the photosynthetic/respiratory electron transport chain, being fuelled by electrons donated from NADPH or ferredoxin, which are subsequently transferred to the plastoquinone pool (Price *et al.*, 2002). After the hydration of CO_2, a proton is thought to be released into the thylakoid lumen, contributing to the pH gradient necessary for ATP synthesis and making the reaction irreversible in the light (Price *et al.*, 2002).

Conversion of CO_2 to HCO_3^- by the NDH complex has been proposed to drive internal C_i recycling to minimize loss via CO_2 efflux (Maeda *et al.*, 2002; Price *et al.*, 2002). Due to the strong CO_2 accumulation required in cyanobacteria, CO_2 efflux is a major challenge in these organisms. Despite the interplay of the carboxysome and proposed recapture of CO_2 by the NDH-1_4 complex, efflux of CO_2 has been shown to equal ~50–90% of gross C_i uptake in *Trichodesmium* (Kranz *et al.*, 2009; Kranz *et al.*, 2010). Next to the C source (CO_2 vs HCO_3^-), leakage (i.e. CO_2 efflux : gross C_i uptake) can strongly affect isotopic composition of organic C produced during photosynthesis (Burkhardt *et al.* 1999, Sharkey and Berry, 1985), and thus measurements of ^{13}C fractionation can provide complementary information on this aspect of CCM regulation (e.g. Laws *et al.*, 1997; Keller and Morel, 1999; Rost *et al.*, 2006; Tchernov and Lipschultz, 2008). In fact, differences in leakage estimates based on membrane inlet mass spectrometry (MIMS; Badger *et al.*, 1994) and C isotope fractionation (Sharkey and Berry, 1985) have been attributed to internal C_i cycling driven by NDH (Kranz *et al.*, 2010).

In a previous study (Eichner *et al.*, 2014), the energy allocation to different physiological processes in *Trichodesmium* under varying energetic states was addressed by altering the cellular energy budget through addition of different nitrogen sources: while N_2 fixation is a highly energy-demanding process with a high demand for ATP, NO_3^- requires very little ATP (only for uptake) but instead has a high electron demand. The study highlighted the dependence of energy reallocation on the stoichiometry in energy demands (ATP vs NADPH) of the different pathways involved. The energy demand of the CCM in *Trichodesmium* remains uncertain, however, especially because the regulation of internal C_i fluxes is as yet poorly characterized. To shed light on the extra- and intracellular C_i fluxes under the different energetic conditions, *Trichodesmium* was grown with different pCO_2 levels and N sources (N_2 vs NO_3^-), and a combination of different methods, including MIMS and ^{13}C fractionation measurements, as well as modelling, was employed. While MIMS provides a useful tool to investigate C_i fluxes across the cell membrane, internal fluxes cannot be directly measured and were therefore modelled. Model calculations of internal C_i fluxes made use of the measured extracellular C_i fluxes and the isotopic composition of particulate organic C ($\delta^{13}C_{POC}$), which reflects the integrated effects of extra- and intracellular C_i fluxes. Hereby, a common model of ^{13}C fractionation (Sharkey and Berry, 1985) was extended by including internal fluxes around the carboxysome.

Materials and methods

Culture conditions

Trichodesmium erythraeum IMS101 was grown in semi-continuous batch cultures at 25°C and 150 µmol photons m^{-2} s^{-1} with a 12 h : 12 h light : dark cycle. Cultures were grown in 0.2-µm-filtered artificial seawater (YBCII medium; Chen *et al.*, 1996) and kept in exponential growth phase by regular dilution with culture medium. Culture bottles were continuously bubbled with 0.2-µm-filtered air with pCO_2 levels of 380 and 1400 µatm. Prior to experiments, cells were allowed to acclimate to the respective pCO_2 for at least 2 weeks. Cultures in which pH had drifted by >0.09 units compared to cell-free reference media were excluded from further analysis. In treatments with NO_3^- as the N source, 0.2-µm-filtered $NaNO_3$ was added to achieve mean concentrations of 97 ± 2 µmol l^{-1} in the experiments, and these never

fell below 65 µmol l^{-1}. Cultures were acclimated to NO_3^- for at least 1 week before measurements. Samples for the analysis of dissolved inorganic C (DIC) were filtered through 0.2 µm filters and measured colourimetrically (QuAAtro autoanalyzer, Seal, Norderstedt, Germany). Average precision was ±5 µmol kg^{-1}. The pH values of the acclimation media were measured potentiometrically (pH meter pH3110, WTW, Weilheim, Germany). For further details on culture conditions as well as carbonate chemistry parameters, see Eichner *et al.* (2014).

MIMS measurements

Cellular C_i fluxes (Fig. 1) were obtained using a custom-made MIMS system (Rost *et al.*, 2007), applying a disequilibrium approach described by Badger *et al.* (1994). Assays were performed in YBCII medium buffered with HEPES (50 mM, pH 8.0) at acclimation temperature and light intensity, unless otherwise specified. To account for the diurnal cycle of C_i fluxes in *Trichodesmium*, measurements were performed three times over the day, during time intervals from 0 to 1.5, 5.5 to 7, and 9 to 10.5 h after beginning of the photoperiod. CO_2 and O_2 fluxes were measured as a function of DIC, starting with concentrations close to zero (media bubbled with CO_2-free air), which were subsequently increased by step-wise addition of $NaHCO_3$ up to concentrations of ~5000 µM. As the assay medium is buffered, unlike the conditions during acclimation of the cells, the HCO_3^-:CO_2 ratio stayed constant over the investigated DIC range. DIC-saturated rates of photosynthesis (V_{max}) and half-saturation concentrations [$K_{1/2}$ (DIC)] were obtained by fitting a Michaelis-Menten function to the data. Net O_2 evolution was converted to C fixation (F_{fix}) assuming a photosynthetic quotient (PQ) of 1.34 (Williams and Robertson, 1991). Net CO_2 uptake ($F_{cyt,\ netCO2}$) was calculated from the steady-state rate of CO_2 depletion at the end of the light period and corrected for the CO_2/HCO_3^- interconversion in the medium ($F_{ext,\ db}$). Using C fixation and net CO_2 uptake, HCO_3^- uptake rates ($F_{cyt,\ HCO3-}$) could be derived by a mass balance equation:

$$F_{cyt,HCO_3^-} = F_{fix} - F_{cyt,netCO_2} \quad (1)$$

For normalization of the CO_2 and O_2 traces, duplicate samples for chlorophyll *a* (chl *a*) analysis were taken after each measurement. Chl *a* was extracted in acetone for >12 h and determined fluorometrically (TD-700 fluorometer, Turner Designs, Sunnyvale, CA, USA; Holm-Hansen and Rieman, 1978).

Leakage estimation

Cellular leakage was estimated by two different methods. Firstly, leakage was determined by MIMS measurements using the disequilibrium approach (Badger *et al.*, 1994). Cellular leakage (L_{MIMS}) is defined as the ratio of CO_2 efflux ($F_{cyt,\ out}$) to gross C_i uptake [i.e. the sum of HCO_3^- ($F_{cyt,\ HCO3-}$) and gross CO_2 uptake ($F_{cyt,\ CO2}$)]:

$$L_{MIMS} = \frac{F_{cyt,out}}{F_{cyt,HCO_3^-} + F_{cyt,CO_2}} \quad (2)$$

$F_{cyt,\ out}$ was estimated from the initial increase in CO_2 concentration after switching off the light (Badger *et al.*, 1994). These estimates are based on the assumption that the rate of diffusive CO_2 efflux during the light phase is well represented by the rate of CO_2 efflux during the first ~20 s of the subsequent dark phase. As leakage calculated by this approach is based on O_2 measurements that are converted to C fluxes, the sensitivity to different PQ values was tested by varying PQ between 1.0 and 1.7, yielding deviations of not more than 15% of leakage estimates (i.e. 0.06 units).

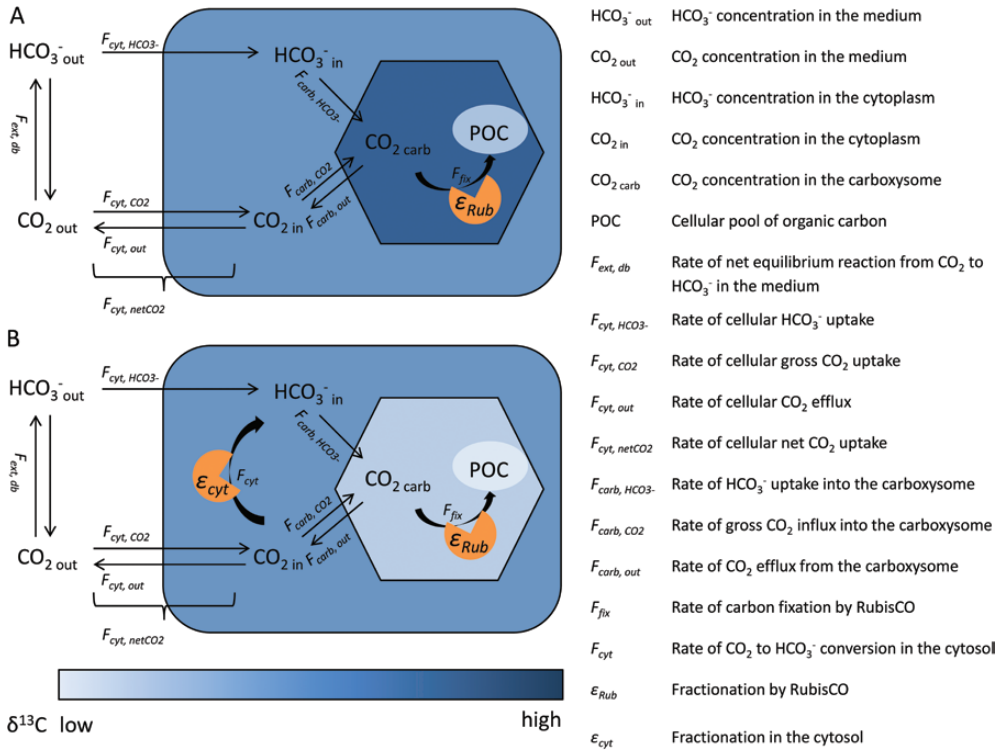

Fig. 1. Schematic diagram showing the cellular C_i pools and fluxes characterized by measurements and modelling. Fluxes and concentrations in the external medium and fluxes over the cell membrane as well as C fixation (F_{fix}) were measured by MIMS, while fluxes in and out of the carboxysome were modelled. Shading intensity denotes $\delta^{13}C$ values of different cellular C pools (including POC and C_i in the cytosol and carboxysome). (A) Fractionation during C fixation by RubisCO leads to depletion of POC in ^{13}C and enrichment of ^{13}C in the carboxysomal C_i pool. (B) Fractionation during internal C_i cycling, e.g. via NDH, leads to ^{13}C depletion of the carboxysomal C_i pool. Consequently, the POC formed is isotopically lighter than in scenario A. This figure is available in colour at *JXB* online.

In the second approach, leakage was estimated from the isotopic fractionation during POC formation (ε_p), which was calculated from the difference in isotopic composition between POC ($\delta^{13}C_{POC}$) and CO_2 ($\delta^{13}C_{CO2}$) in the medium according to Freeman and Hayes (1992). Duplicate samples for analysis of $\delta^{13}C_{POC}$ were filtered onto pre-combusted GF/F filters and acidified with 200 µl HCL (0.2 M) to remove all C_i prior to analysis. $\delta^{13}C_{POC}$ was measured with an EA mass spectrometer (ANCA SL 2020, SerCon Ltd, Crewe, UK). For analysis of the isotopic composition of DIC ($\delta^{13}C_{DIC}$), filtered samples were fixed with $HgCl_2$ (final concentration 110 mg l^{-1}). Subsequent to acidification of the samples, isotopic composition of CO_2 in the headspace was analysed with an isotope ratio mass spectrometer (GasBench-II coupled to Delta-V advantage, Thermo, Bremen, Germany). The isotopic composition of CO_2 was calculated from $\delta^{13}C_{DIC}$, following a mass balance equation (Zeebe and Wolf-Gladrow, 2007). Leakage (L_{13C}) was subsequently derived using an extended equation from Sharkey and Berry (1985):

$$L_{13C} = \frac{\varepsilon_p - (a_{cyt}\varepsilon_{db})}{\varepsilon_{Rub}} \quad (3)$$

where ε_{Rub} is the intrinsic discrimination of ^{13}C by RubisCO (assumed to be +25‰; Roeske and O'Leary, 1984; Guy *et al.*, 1993) and ε_{db} represents the equilibrium fractionation between CO_2 and HCO_3^- (–9‰; Mook *et al.*, 1974). The fractional contribution of HCO_3^- to gross C_i uptake (a_{cyt}), being introduced by Burkhardt *et al.* (1999), has been determined by MIMS measurements for the respective treatments. These calculations assume an equilibrium situation and further consider the cell as a single compartment.

Results and discussion

General CCM characteristics

MIMS measurements showed a highly efficient CCM with a high capacity for regulation of C_i affinity over the diurnal cycle as well as with different pCO_2 levels, in agreement with previous studies on *Trichodesmium* (e.g. Kranz *et al.*, 2009; Kranz *et al.*, 2010). Half-saturation DIC concentrations for C fixation ($K_{1/2}$) ranged between ~20 and 500 µmol DIC l^{-1} (Supplementary Figure S1), which is equivalent to ~0.2 and 4 µmol CO_2 l^{-1} and is thus substantially lower than the K_M of cyanobacterial RubisCO (105–185 µmol CO_2 l^{-1}; Badger *et al.*, 1998). Taking the ratio of K_M to $K_{1/2}$ as a measure of CO_2 accumulation in the vicinity of RubisCO (assuming a K_M of 150 µmol CO_2 l^{-1}), our data suggest accumulation factors between ~35 and 900 and indicate that the degree of RubisCO saturation is always larger than 80%. Accordingly, under the applied external CO_2 concentrations, concentrations in the carboxysome typically exceed 600 µmol CO_2 l^{-1}. The CCM was primarily based on active HCO_3^- uptake, accounting for 82 ± 4% of gross C_i uptake (Table 1). As gross C_i uptake was approximately twice as high as net C fixation at acclimation DIC (~2100 µmol CO_2 l^{-1}), leakage measured by MIMS ranged between 0.3 and 0.7 (i.e. CO_2 efflux equalled 30–70% of gross C_i uptake; Table 1). As a consequence of the high HCO_3^- contribution and the high CO_2 efflux, the net fluxes of CO_2 were generally directed out of the cell (cf. negative values for net CO_2 uptake: Table 1, Fig. 2).

Diurnal changes in C_i fluxes

The diurnal cycle was characterized by low $K_{1/2}$ values in the morning and a downregulation of C fixation rates at midday (ANOVA, $P < 0.001$; Supplementary Figure S1A and B). Leakage estimated by MIMS at acclimation DIC was lowest in the morning, increased towards midday, and decreased again towards the evening (ANOVA, $P < 0.05$; Table 1). Leakage estimates for DIC levels approaching zero (obtained by curve fits of leakage plotted over DIC concentration; Fig. 2) varied even more over the course of the day, yielding values around 0.3 in the mornings, while at midday and in the evening ratios approached 1.0 (data not shown). These diurnal changes in leakage could be explained by the concurrent changes in the ratio of HCO_3^- to CO_2 uptake (Table 1, Supplementary Figure 1C), which were characterized by low CO_2 fluxes in the mornings (ANOVA, $P < 0.05$; Table 1), while HCO_3^- uptake was higher in the morning than at midday, and increased again towards the evening (ANOVA, $P < 0.05$; Table 1). Over the day, a higher share of HCO_3^- uptake, which is less prone to diffuse out of the cell, was thus correlated with lower leakage.

Effects of different pCO_2 levels and N sources

The affinity for C_i was downregulated at elevated pCO_2, as indicated by high $K_{1/2}$ values under these conditions (Supplementary Figure 1B). Under acclimation DIC, however, C_i fluxes (C fixation, C_i uptake, and CO_2 uptake and efflux) were not

Table 1. *Diurnal cycle of C_i fluxes measured by MIMS under acclimation DIC levels (~2100 µmol l^{-1}) in* Trichodesmium *acclimated to two different pCO_2 levels (380 vs 1400 µatm) and N sources (N_2 vs NO_3^-)*[a]

	380 µatm –NO_3^-			380 µatm +NO_3^-			1400 µatm –NO_3^-			1400 µatm +NO_3^-		
	Morning	Midday	Evening	Morning	Midday	Evening	Morning	Midday	Evening	Morning	Midday	Evening
Net C fixation	91 ± 15	57 ± 14	87 ± 3	95 ± 20	56 ± 22	70 ± 18	80 ± 13	39 ± 14	61 ± 4	91	61 ± 19	63 ± 16
Gross C_i uptake	157 ± 18	144 ± 24	167 ± 17	135 ± 23	128 ± 16	143 ± 25	144 ± 7	124 ± 9	142 ± 6	144	127 ± 22	131 ± 17
HCO_3^- uptake	134 ± 18	117 ± 22	133 ± 12	118 ± 21	108 ± 14	113 ± 14	126 ± 11	95 ± 9	112 ± 2	120	97 ± 17	102 ± 12
Gross CO_2 uptake	23 ± 4	27 ± 4	34 ± 6	17 ± 3	20 ± 2	30 ± 13	18 ± 4	28 ± 5	30 ± 6	24	30 ± 9	29 ± 6
Net CO_2 uptake	–45 ± 10	–60 ± 12	–46 ± 9	–23 ± 2	–52 ± 8	–42 ± 11	–46 ± 5	–56 ± 8	–51 ± 4	–28	–36 ± 8	–39 ± 9
HCO_3^-:C_i uptake	0.85 ± 0.03	0.81 ± 0.03	0.80 ± 0.02	0.87 ± 0.01	0.84 ± 0.01	0.80 ± 0.06	0.88 ± 0.03	0.77 ± 0.04	0.79 ± 0.03	0.83	0.76 ± 0.05	0.78 ± 0.01
CO_2 efflux	69 ± 12	87 ± 13	79 ± 13	40 ± 3	72 ± 6	72 ± 8	64 ± 7	85 ± 14	81 ± 3	53	66 ± 4	67 ± 10
Leakage	0.44 ± 0.05	0.61 ± 0.05	0.47 ± 0.03	0.30 ± 0.03	0.57 ± 0.11	0.51 ± 0.04	0.45 ± 0.07	0.69 ± 0.10	0.57 ± 0.01	0.37	0.53 ± 0.07	0.52 ± 0.07

[a] All C_i fluxes are given in µmol C (mg chl *a*)$^{-1}$ h^{-1}. Errors are standard deviations for biological replicates (1 SD; $n = 3$ except 1400 +NO_3^- morning with $n = 1$).

significantly affected by pCO_2 (ANOVA, $P > 0.05$; Table 1), reflecting the cells' capacity to achieve similar C fixation over a range of pCO_2 levels by regulating their CCM. Regarding the N source, C fixation rates and CO_2 uptake under acclimation DIC were equally unaffected (ANOVA, $P > 0.05$; Table 1). Although cells mainly used HCO_3^- as a C_i source in all treatments, HCO_3^- uptake at acclimation DIC decreased slightly with increasing pCO_2 (~10%; ANOVA, $P < 0.05$; Table 1, Supplementary Figure 1C), but was not affected by N source (ANOVA, $P > 0.05$; Table 1). Interestingly, CO_2 efflux was affected by the N source (ANOVA, $P < 0.01$; Table 1), with ~20% lower efflux in NO_3^- users compared to N_2 fixers, possibly due to differences in internal pH caused by the uptake/accumulation of NO_3^- vs NH_4^+ in the cell. One could also speculate that growing cells on NO_3^- reduces the general membrane permeability, since NH_4^+ transfer between cells is only necessary under N_2-fixing conditions, which could also affect the permeability for CO_2. Leakage at acclimation DIC estimated by MIMS was, however, not significantly affected by pCO_2 or N source at any time of the day (ANOVA, $P > 0.05$; Table 1).

Offsets in leakage estimates

High leakage values obtained in MIMS measurements reflect the strong C_i accumulation necessary for C fixation in cyanobacteria due to the poor CO_2 affinity of their RubisCO. However, leakage estimates obtained from $\delta^{13}C$ values (L_{13C}, eqn 3) even exceeded MIMS-based estimates. Overall fractionation during formation of POC (ε_p) was not significantly affected by N treatment (ANOVA, $P > 0.05$) but increased with pCO_2 (ANOVA, $P < 0.0001$), ranging from 14.4 ± 1.0‰ at 380 µatm to 19.9 ± 0.9‰ at 1400 µatm pCO_2. Consequently, leakage estimates based on ε_p (eqn 3) also increased with pCO_2, while estimates from MIMS measurements at acclimation DIC were constant over the range of pCO_2 levels. L_{13C} was calculated to range between 0.82 and 1.14, exceeding MIMS-based measurements by ~30–60% (Fig. 3) and even reaching theoretically impossible values (>1). A similar discrepancy between these two approaches, which was equally dependent on pCO_2 acclimation, has been observed previously (Kranz *et al.*, 2010). In the following paragraph, possible reasons for the deviations between estimates are outlined.

Following the approach by Badger *et al.* (1994), leakage is directly calculated from the measured CO_2 efflux and gross C_i uptake. As CO_2 efflux cannot readily be determined during the light due to the concurrent C_i uptake, the rise in the CO_2 signal directly after switching off the light is taken as an estimate of CO_2 efflux during the light phase, assuming that the accumulated C_i pool and therewith gross CO_2 efflux are initially at the pre-darkness level (Badger *et al.*, 1994). If active C_i uptake as well as C fixation by RubisCO do not cease immediately upon darkening, leakage estimates could be biased and likely to be underestimated. Despite these potential uncertainties, this is a more direct approach than the alternative method, which infers leakage from the isotopic composition of cells. The ^{13}C-based approach makes use of the effect of leakage on ε_p (eqn 3; Sharkey and Berry, 1985). Briefly, while the intrinsic fractionation by RubisCO (ε_{Rub}) generally causes organic material to be depleted in ^{13}C (Fig. 1A), variation in ε_p can be induced by changes in the C_i source and/or leakage. Consequently, any errors in

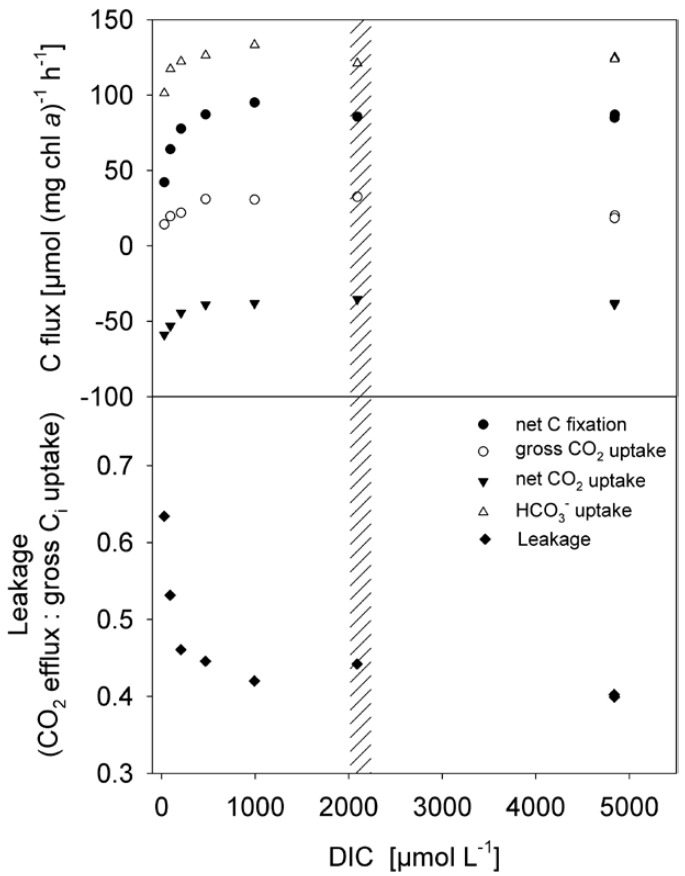

Fig. 2. Example showing the dependence of C_i fluxes measured by MIMS in *Trichodesmium* on the DIC concentration in the assay. Data shown were measured in the evening in a culture grown at 380 µatm pCO_2 without NO_3^-. The shaded area denotes the range of acclimation DIC levels.

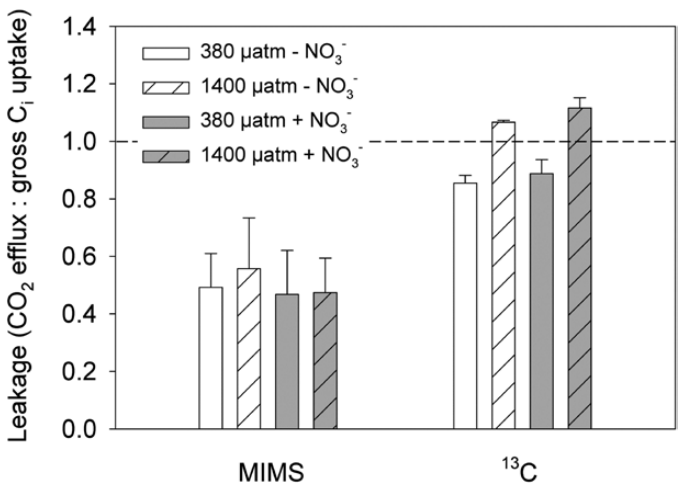

Fig. 3. Leakage estimates by MIMS (mean values of measurements conducted at three time points over the day; Badger *et al.*, 1994) and ^{13}C fractionation (Sharkey and Berry, 1985) determined in *Trichodesmium* grown under two pCO_2 levels and N sources ($n \geq 3$).

estimates of ε_{Rub} or a_{cyt}, but also any unaccounted process affecting ε_p, would cause ^{13}C-based leakage estimates to be biased.

Kranz *et al.* (2010) suggested that internal C_i cycling within the cell may affect ε_p in general. The CO_2 dependence of the offset between MIMS- and ^{13}C-based leakage estimates was furthermore suggested to reflect a CO_2 effect on the NDH complex driving this internal C_i cycling (Kranz *et al.*, 2010), in line with early observations of the C_i dependence of CO_2 uptake by the NDH complex (Price and Badger, 1989a,c). In Fig. 1, the effects of internal C_i cycling on isotopic composition are illustrated. While Fig. 1A assumes an equilibrium situation and does not include any internal C_i cycling, Fig. 1B illustrates non-equilibrium situations caused by internal C_i cycling. The degree of ^{13}C enrichment in the cytosol and within the carboxysome, according to this concept, would be dependent on the type of kinetic fractionation in the cytosol. This could include complete or incomplete unidirectional fractionation as well as enzymatic fractionation by the NDH complex. Accounting for these processes requires the introduction of a second compartment. The approach taken here can be considered as an extension of the model of Sharkey and Berry (1985), which considers the cell as one compartment. In order to avoid errors being introduced by large uncertainties, e.g. in permeability of the plasma membrane and carboxysome in *Trichodesmium*, a flux-based model that is independent of these assumptions is employed, rather than a full kinetic model. Our approach is similar to the model of Schulz *et al.* (2007), but disequilibrium situations are also considered.

Internal C_i fluxes and fractionation—model setup

To test our concept (Fig. 1) and quantitatively describe the possible effect of internal cycling on $\delta^{13}C$, intracellular C_i fluxes and their effects on isotopic ratios in different cellular C_i pools were modelled. For parameterizations, HCO_3^- and gross CO_2 fluxes measured by MIMS as well as measured fractionation values ε_p were used. The model is based on flux balance equations for the individual isotope species. The flux balance of total C (^{12}C + ^{13}C) in the cytosol and in the carboxysome, respectively, is given by the following equations:

$$F_{cyt,CO_2} + F_{cyt,HCO_3^-} + F_{carb,out} - F_{cyt,out} - F_{carb,CO_2} - F_{carb,HCO_3^-} = 0 \quad (4)$$

$$F_{carb,HCO_3^-} + F_{carb,CO_2} - F_{carb,out} - F_{fix} = 0 \quad (5)$$

As about 99% of C is ^{12}C, i.e. $F = {}^{12}F + {}^{13}F \equiv {}^{12}F$, the flux balance equations for ^{13}C can be derived by multiplying the fluxes (F) with the isotopic ratio $R = {}^{13}C/{}^{12}C$. The isotopic fractionation factor α_{db} is defined by the isotopic ratio of CO_2 divided by the isotopic ratio of HCO_3^-, i.e. $\alpha_{db} = R_{CO_2} / R_{HCO_3^-}$. Using the equilibrium fractionation (ε_{db}), the fractionation factor between CO_2 and HCO_3^- can be calculated for the external medium as well as for the cytosol according to:

$$\alpha_{db,ext} = 1 + \varepsilon_{db}/1000 \quad (6)$$

$$\alpha_{db,cyt} = 1 + \varepsilon_{cyt}/1000 \quad (7)$$

While the equilibrium value ε_{db} is –9‰ (i.e. CO_2 is isotopically lighter than HCO_3^-; Mook *et al.*, 1974), ε_{cyt} can significantly deviate from this value due to kinetic effects. The uncatalysed conversion of HCO_3^- to CO_2 shows a kinetic fractionation of –22‰, whereas the formation of HCO_3^- from CO_2 is associated with a kinetic fractionation of +13‰ (Marlier and O'Leary, 1984). Hence, the actual value of ε_{cyt} is determined by the disequilibrium between CO_2 and HCO_3^- in the cytosol, which depends on all fluxes in and out of the cytosol, and on the internal CO_2 and HCO_3^- concentrations, which cannot be calculated in the framework of a flux-based model. Assuming a unidirectional conversion of CO_2 to HCO_3^- in the cytosol, a value of +13‰ for ε_{cyt} will be adopted. By setting ε_{cyt} to +30‰, a potential fractionation by the NDH-1_4 complex will be taken into account. The situation where the conversion of CO_2 to HCO_3^- in the cytosol is not completely unidirectional will be considered by setting ε_{cyt} to +8‰.

The R associated with F_{fix} can be written in terms of the isotopic fractionation against ^{13}C by RubisCO described by the factor $\alpha_{Rub} = R_{carb} / R_{POC}$, where R_{carb} is the isotopic ratio of CO_2 in the carboxysome and R_{POC} is the isotopic ratio of POC. The value of α_{Rub} is calculated from the intrinsic RubisCO fractionation ε_{Rub} (assuming an intermediate value of +25‰; Roeske and O'Leary, 1984; Guy *et al.*, 1993):

$$\alpha_{Rub} = 1 + \varepsilon_{Rub}/1000 \quad (8)$$

Given the isotopic ratios (R) of CO_2 and the isotopic fractionation factors between HCO_3^- and CO_2 expressed as $\alpha_{bd} = 1/\alpha_{db}$, the flux balance equations for ^{13}C can be derived from eqns 4 and 5 for the cytosol and the carboxysome, respectively:

$$R_{ext}F_{cyt,CO_2} + \alpha_{bd,ext}R_{ext}F_{cyt,HCO_3^-} + R_{carb}F_{carb,out} - R_{cyt}F_{cyt,out} - R_{cyt}F_{carb,CO_2} - \alpha_{bd,cyt}R_{cyt}F_{carb,HCO_3^-} = 0 \quad (9)$$

$$\alpha_{bd,cyt}R_{cyt}F_{carb,HCO_3^-} + R_{cyt}F_{carb,CO_2} - R_{carb}F_{carb,out} - R_{carb}F_{fix}/\alpha_{Rub} = 0 \quad (10)$$

R_{cyt} is the isotopic ratio of CO_2 in the cytosol. The overall isotopic fractionation by the cell is defined with respect to the isotopic composition of CO_2 in the external medium (R_{ext}):

$$\varepsilon_p = \left(\frac{R_{ext}}{R_{POC}} - 1\right) \times 1000 = \left(\alpha_{Rub}\frac{R_{ext}}{R_{carb}} - 1\right) \times 1000 \quad (11)$$

The ratio R_{ext}/R_{carb} reflects the impact of the inner compartment on the isotopic fractionation and can be calculated from flux balance eqns 9 and 10. Eqn 10 can be solved for R_{cyt}, which in turn is substituted into eqn 9, yielding the ratio:

$$\frac{R_{ext}}{R_{carb}} = \frac{\left(F_{fix}/\alpha_{Rub} + F_{carb,out}\right)\left(F_{carb,CO_2} + \alpha_{bd,cyt}F_{carb,HCO_3^-} + F_{cyt,out}\right)}{\left(F_{cyt,CO_2} + \alpha_{bd,ext}F_{cyt,HCO_3^-}\right)\left(F_{carb,CO_2} + \alpha_{bd,cyt}F_{carb,HCO_3^-}\right)} - \frac{F_{carb,out}}{\left(F_{cyt,CO_2} + \alpha_{bd,ext}F_{cyt,HCO_3^-}\right)} \quad (12)$$

$$= \frac{F_{cyt,out}}{\alpha_{Rub}\left(F_{cyt,CO_2} + \alpha_{bd,ext}F_{cyt,HCO_3^-}\right)} \times \left(\frac{F_{fix}}{F_{cyt,out}} + \frac{F_{fix} + \alpha_{Rub}F_{carb,out}}{F_{carb,CO_2} + \alpha_{bd,cyt}F_{carb,HCO_3^-}}\right)$$

This solution is valid for arbitrary combinations of fluxes as long as the constraints imposed by flux balance equations 4 and 5 are obeyed:

$$\begin{aligned} F_{fix} &= F_{carb,CO_2} + F_{carb,HCO_3^-} - F_{carb,out} \\ &= F_{cyt,CO_2} + F_{cyt,HCO_3^-} - F_{cyt,out} \end{aligned} \quad (13)$$

Given the fractional contribution of HCO_3^- to total C_i uptake into the cytosol (a_{cyt}) and the carboxysome (a_{carb}), as well as the leakage out of the cytosol (L_{cyt}) and the carboxysome (L_{carb}), eqns 6 to 8 and 11 to 13 can be used to derive the overall isotopic fractionation:

$$\begin{aligned} \varepsilon_p &= \frac{a_{cyt}\varepsilon_{db}}{1 - a_{cyt}\varepsilon_{db}/10^3} + L_{cyt}\frac{\left(a_{carb}\varepsilon_{\mathrm{cyt}} + L_{carb}\varepsilon_{Rub}\right)}{\left(1 - a_{cyt}\varepsilon_{db}/10^3\right)\left(1 - a_{carb}\varepsilon_{cyt}/10^3\right)} \\ &\approx a_{cyt}\varepsilon_{db} + L_{cyt}\left(a_{carb}\varepsilon_{cyt} + L_{carb}\varepsilon_{Rub}\right). \end{aligned} \quad (14)$$

Solving the approximated solution for L_{cyt} yields the following:

$$L_{cyt} = \frac{\varepsilon_p - a_{cyt}\varepsilon_{db}}{a_{carb}\varepsilon_{cyt} + L_{carb}\varepsilon_{Rub}} \quad (15)$$

The approximate solution can be considered as a generalization of the original function given by Sharkey and Berry (1985), accounting for two compartments. The authors assumed that the cell takes up HCO_3^- into a single compartment and subsequently converts it to CO_2; hence there is no HCO_3^- inside the cell. The compatibility of our model with the original function can be confirmed by comparing ε_p for $L_{carb} = 1$ (i.e. no second compartment) and $a_{carb} = 0$ (i.e. only CO_2 uptake into the carboxysome).

As pointed out by Schulz *et al.* (2007), diffusive CO_2 fluxes generally need to be added to cellular fluxes measured by MIMS (Badger *et al.*, 1994) when relating them to ^{13}C fractionation. For membrane permeability exceeding 10^{-4} cm s^{-1}, as proposed for a diatom (~10^{-2} cm s^{-1}; Hopkinson *et al.*, 2011), diffusive CO_2 fluxes are high and internal CO_2 concentrations approach those of the cell's exterior (Supplementary Figure S2). In this case, gross CO_2 efflux estimated by MIMS would be underestimated, which could explain part of the discrepancy between MIMS-based leakage and estimates based on eqn 4 (Sharkey and Berry, 1985). While there is, to our knowledge, no recent data on the membrane permeability of cyanobacteria available, older studies on cyanobacteria state significantly lower values, approaching 10^{-5} cm s^{-1} (Badger *et al.*, 1985; Marcus *et al.*, 1986), which are in line with diffusive CO_2 fluxes being low enough to allow for considerable CO_2 accumulation in the cell (Supplementary Figure S2). Using this permeability, the effect of diffusive CO_2 influx on leakage obtained by our model was estimated, yielding maximum changes in the order of a few percent, which were thus neglected. In view of the uncertainties in this parameter, measurements of membrane permeability of cyanobacteria are needed to improve future estimates of internal C fluxes.

Internal C_i fluxes and fractionation—model application

To test the sensitivity of our model, the potential effect of changes in a_{cyt} on ε_p was quantified, using the maximum variability observed in our study (0.84 vs 0.76) while leaving all other parameters constant. This variability can explain a change in ε_p by not more than 0.7‰. Thus, a_{cyt} can be excluded as a main driver behind the variability in ε_p (or leakage estimates), even if variability in a_{cyt} is severely underestimated. Applying the model to our measured fluxes and ε_p values, a range of different possible scenarios for intracellular fluxes and fractionation in the cytosol is obtained (Fig. 4).

According to these interrelations, while at L_{cyt} according to our MIMS measurements (0.5), only a very high fractionation in the cytosol (ε_{cyt}) can explain our results, at $L_{cyt} \geq 0.7$, there is a large range of possible combinations of parameters (see shaded areas in Fig. 4). As we aim to find parameters that can explain ε_p in both of our pCO_2 treatments, the high ε_p measured in cells grown at 1400 µatm constrains the range of possible values, while ε_p of cells grown at 380 µatm could be explained by a larger range of values for a_{carb} and L_{carb} (Fig. 4). High values for a_{carb} and L_{carb} (both approaching 1) allow for a larger range of possible values of ε_{cyt} to explain our measured ε_p (Fig. 4). Due to the high contribution of HCO_3^- to C_i uptake and the additional conversion of CO_2 to HCO_3^- by the NDH complex, a_{carb} is likely to be close to 1, most probably exceeding a_{cyt} measured in our experiment (0.82). Moreover, high diffusive CO_2 influx into the carboxysome seems unlikely in view of the supposed function of the carboxysome as a diffusion barrier to CO_2 (e.g. Reinhold *et al.*, 1989). While comparison experiments with CA knockout mutants with intact and broken carboxysomes confirmed that the carboxysome shell impedes diffusion of CO_2 (Dou *et al.*, 2008), the pores in the hexamer protein subunits of the shell are supposed to

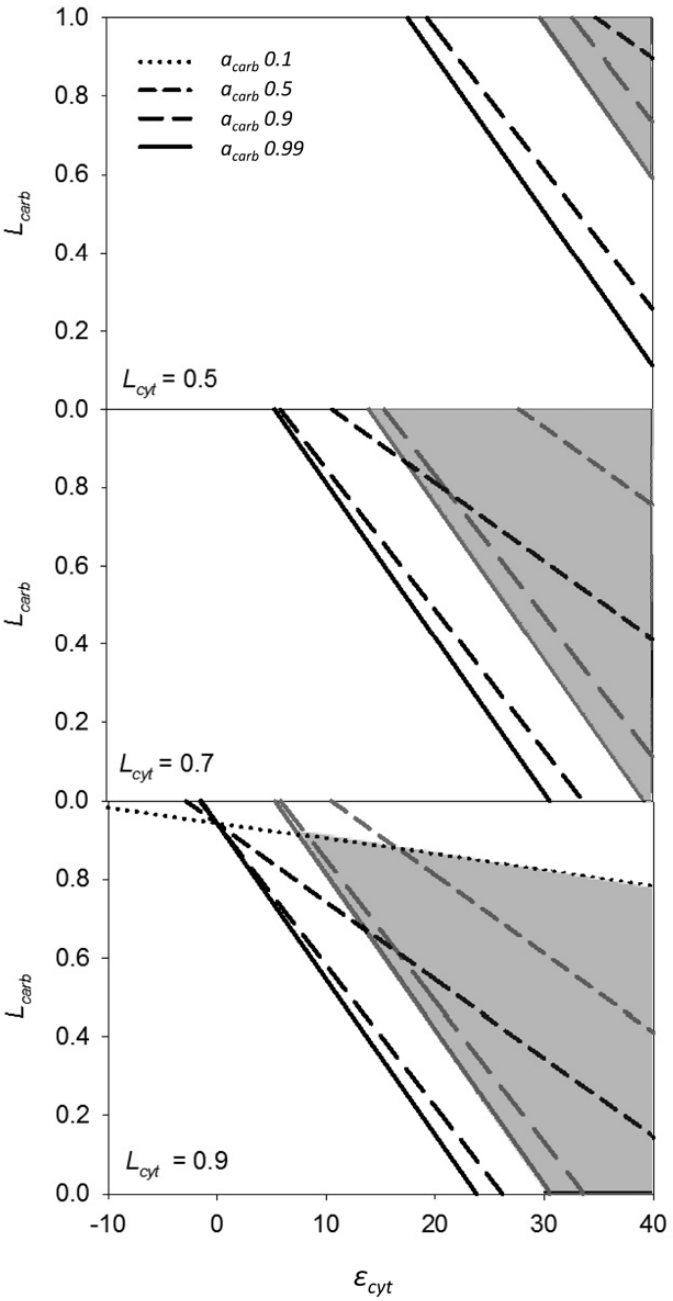

Fig. 4. Interrelationship between L_{carb}, ε_{cyt}, and a_{carb} in the model, depicted for different values of L_{cyt} and ε_p. The shaded areas mark the range of possible values for L_{carb} and ε_{cyt} that could reconcile our measurements of isotopic composition with measured external C_i fluxes. Black and grey lines are based on ε_p measured in cells acclimated to 380 and 1400 µatm pCO_2, respectively.

be permeable to small, negatively charged molecules such as HCO_3^- (Tsai *et al.*, 2007; Klein *et al.*, 2009; Espie and Kimber, 2011). Despite the low CO_2 permeability, high rates of CO_2 efflux, and thus high L_{carb}, are likely due to the very high accumulation factor (two to three orders of magnitude; this study and Kaplan *et al.*, 1980). A value for L_{carb} of 0.9 is therefore used in the model scenarios described in the following (Table 2). Using eqn 13, the following expression for the ratio of internal to external C_i fluxes can be derived:

Table 2. *Different scenarios of external and internal C_i fluxes that can reconcile measurements of C_i fluxes by MIMS and ε_p values obtained in this study (scenarios 1, 2 and 4 to 6) and by Kranz et al. (2010, scenario 3)*[a]

Scenario	pCO_2	ε_p	a_{cyt}	L_{MIMS}	L_{13C}	L_{cyt}	L_{carb}	a_{carb}	ε_{cyt}
		Measured				Modelled			
1	1400	20	0.8	0.5	1.1	0.8	0.9	1	13
2	380	14	0.8	0.5	0.8	0.6	0.9	1	13
3	180	7	0.8	0.4	0.6	0.4	0.9	1	13
4	1400	20	0.8	0.5	1.1	0.9	0.9	1	8
5	1400	20	0.8	0.5	1.1	0.5	0.9	1	30
6	380	14	0.8	0.5	1.1	0.6	0.9	0.7	20

[a]ε_p, a_{cyt}, and L_{MIMS} were measured; L_{13C} was calculated from ε_p according to Sharkey and Berry (1985); remaining values are model input parameters and model results (L_{cyt}, L_{carb}, a_{carb}, and ε_{cyt}).

$$\frac{F_{carb,CO_2} + F_{carb,HCO_3^-}}{F_{cyt,CO_2} + F_{cyt,HCO_3^-}} = \frac{1 - L_{cyt}}{1 - L_{carb}} \quad (16)$$

For the chosen value for L_{carb} of 0.9 and the measured L_{cyt} of 0.5, eqn 16 yields a ratio of internal vs external C_i cycling of 5.

Compared to estimates based on Sharkey and Berry (1985), our model significantly improved the compatibility of leakage estimates with those obtained by MIMS measurements (Table 2). The maximum fractionation that could be achieved in an uncatalysed reaction from CO_2 to HCO_3^- is +13‰ (O'Leary *et al.*, 1992). With this kinetic fractionation, ε_p values measured for the two pCO_2 levels can be explained by leakage values from the cytosol (L_{cyt}) of 0.8 and 0.6, respectively (scenarios 1 and 2, Table 2), which are significantly lower than the estimates based on the function by Sharkey and Berry (L_{13C} = 1.1 and 0.8, respectively). The remaining difference to leakage estimates obtained by MIMS (L_{MIMS} = 0.5) could be explained by an underestimation of leakage by the MIMS approach, as discussed above. Assuming that the conversion between CO_2 and HCO_3^- in the cytosol was not completely unidirectional, ε_{cyt} could range between +13‰ and –9‰ (equilibrium fractionation; O'Leary *et al.*, 1992). To simulate this intermediate scenario, an ε_{cyt} of +8‰ is assumed (senario 4, Table 2), yielding an L_{cyt} of 0.9 for the high CO_2 treatment.

Kinetic fractionation could be achieved by the NDH complex or by creation of a strong disequilibrium in the cytosol, minimizing the back-reaction from HCO_3^- to CO_2. Mutants of *Synechococcus* expressing human CA in the cytosol were unable to accumulate C_i (Price and Badger, 1989b), suggesting that HCO_3^- is accumulated in the cytosol, and that a chemical disequilibrium in the cytosol favours the reaction from HCO_3^- to CO_2 rather than the opposite direction. This strongly argues for a fractionating enzyme instead of a purely chemical disequilibrium driving unidirectional CO_2 to HCO_3^- conversion in the cytosol. Assuming that NDH not only drives the unidirectional conversion of CO_2 to HCO_3^- but also discriminates against ^{13}C during the reaction, leakage estimates by our model can be further reconciled with MIMS-based

estimates. In a scenario assuming an upper estimate for ε_{cyt} of +30‰ (scenario 5, Table 2), which is within the range of fractionation measured in other enzymes such as RubisCO, our MIMS-measured data can be reproduced even for the high pCO_2 treatment ($L_{MIMS} = L_{cyt} = 0.5$; Table 2). Note that in combination with one of the other factors discussed above, such as an underestimation of L_{carb} or of MIMS-based leakage estimates, enzymatic fractionation less than +30‰ could also explain our measurements (cf. e.g. scenarios with ε_{cyt} of 13‰; Table 2). Although CA and NDH have been proposed to have similar reaction mechanisms (Price *et al.*, 2002), our model results suggest that the fractionation by the NDH complex is different from that of CA (1‰ for conversion of CO_2 to HCO_3^-; Paneth and O'Leary, 1985). This might be due to the fact that the subunit carrying out the hydration reaction in the NDH-1_4 complex (chpX) is embedded in a larger functional unit including the transmembrane proton channel and is associated with the electron transport chain. To confirm the differences in fractionation between these enzyme complexes, however, further work using experimental approaches would be necessary, e.g. by comparing cyanobacterial mutant strains.

Since our MIMS measurements showed that leakage was unaffected by pCO_2 and the slight changes in a_{cyt} could not explain the observed variation in ε_p, a_{carb} and/or ε_{cyt} would need to vary with pCO_2 to explain the observed CO_2-dependence of ε_p. An increase in the activity of the NDH complex could yield an increase in a_{carb} as well as ε_{cyt} and therewith ε_p. With an increase in a_{carb} from 0.7 to 1 and an increase in ε_{cyt} from 20 to 30‰, the measured increase in ε_p between 380 and 1400 µatm can be explained, almost reproducing MIMS-measured leakage in both scenarios (scenarios 5 and 6, Table 2). A higher activity of NDH at high pCO_2 may seem unexpected in view of its supposed role as part of the CCM. However, in contrast to other components of the CCM such as HCO_3^- transporters, the reaction catalysed by the NDH complex contributes to ATP regeneration rather than consuming energy, and thus a downregulation of NDH at high pCO_2 would not provide any energetic benefit to the cell. A positive correlation with pCO_2 might be coupled to the small CO_2 effect on a_{cyt} (Table 1; Supplementary Figure 1C), increasing the activity of the NDH complex at high pCO_2 levels in the acclimations in response to a higher availability of its substrate CO_2. Note that the change in a_{cyt} may have been underestimated in our study due to the constant pH in MIMS measurements. Due to its function as a proton pump in the thylakoid membrane, activity of the NDH complex can increase the ratio of ATP to NADPH available in the cell. The production of ATP by high NDH activity at high pCO_2 could, in turn, contribute to the increased ATP requirement to fuel N_2 fixation in *Trichodesmium* under ocean acidification (e.g. Kranz *et al.*, 2010; Eichner *et al.*, 2014).

Kranz *et al.* (2010) compared leakage estimates based on MIMS and ^{13}C for *Trichodesmium* grown under different pCO_2 levels as well as light intensities. Applying our model to this data set, MIMS-based leakage estimates could be reproduced with unidirectional fractionation for a low pCO_2 treatment with light intensities similar to our experiment (200 µmol photons m^{-2} s^{-1}; scenario 3, Table 2). In high pCO_2 and low light treatments, the difference between L_{MIMS} and L_{cyt} was larger and could consequently only be reconciled with ε_{cyt} values larger than +30‰. Short-term exposure to high light intensities (300 µmol photons m^{-2} s^{-1}) in our experiment affected CO_2 efflux in cells acclimated to high pCO_2 (ANOVA, $P < 0.05$; data not shown). Such light sensitivity generally suggests CO_2 efflux to be closely associated to photosynthetic electron transport. As this light effect was only observed under high pCO_2, i.e. conditions associated with higher NDH activity according to our model results, the interrelation of CO_2 efflux and the NDH complex is further corroborated. The observed light effects on CO_2 efflux (this study) and ε_p (Kranz *et al.*, 2010) impose interesting questions with regard to a potential regulation of the NDH complex by the electron transport chain (redox state and/or proton gradient), which should be investigated in future studies. A better understanding of the regulation of the NDH complex is essential to improve confidence in explaining the effects of pCO_2 as well as light on internal C_i fluxes and potential feedbacks on cellular energy budgets of this key N_2 fixer.

Conclusion and outlook

This study demonstrates that internal C_i fluxes via the NDH-1_4 complex need to be considered not only in terms of cellular C_i acquisition, but also with regard to ^{13}C fractionation and cellular energy status. The comparison of direct measurements of C_i fluxes with estimates based on isotopic composition revealed that ^{13}C fractionation in *Trichodesmium* cannot be adequately described by only considering external C_i fluxes.

Compatibility with direct leakage measurements was improved by applying a model accounting for internal C_i fluxes around the carboxysome, e.g. via the NDH complex, providing a generalization of the model of Sharkey and Berry (1985) applicable for two compartments. In these model calculations, a large fraction of HCO_3^- uptake into the carboxysome (0.7–1, Table 2) and high leakage from the carboxysome (>0.9, Table 2) are assumed, in accordance with the current understanding of carboxysome functioning. A large range of fractionation values for the cytoplasm, representing uncatalysed, unidirectional fractionation as well as enzymatic fractionation by the NDH complex, could significantly improve compatibility of leakage estimates (Table 2), even though the exact interplay of these processes still has to be resolved. While the lack of recent literature data on membrane permeability of cyanobacteria clearly demands future measurements, our model calculations are insensitive to this parameter within a certain range of permeability estimates ($<10^{-4}$ m^{-2} s^{-1}). Similarly, the model is independent of other potentially uncertain assumptions such as permeability of the carboxysome and pH values for the different compartments. Once future studies improve confidence in these parameters, a kinetic model can be used to predict internal concentrations and individual C_i fluxes. The agreement of model results with measured values could further be improved by accounting for possible ^{13}C enrichment of CO_2

leaking out of the cell as well as a disequilibrium situation in the surroundings of the cell (altering the isotopic signature of HCO_3^- taken up).

The model applied here could also be used to improve estimates of leakage based on ^{13}C signatures for other species in which several compartments and/or internal C_i fluxes play an important role. For phytoplankton groups that are relevant in terms of paleo-proxies, this could have important implications for the interpretation of C isotope signals.

Supplementary material

Supplementary Figure S1. DIC-saturated rates of C fixation (V_{max}), half saturation DIC concentrations ($K_{1/2}$) and HCO_3^- : C_i uptake ratios measured at three time points during the day in *Trichodesmium* grown under two pCO_2 levels and N sources (N_2 and NO_3^-).

Supplementary Figure S2. The dependence of intracellular CO_2 concentrations on membrane permeability.

Funding

This work was supported by the European Research Council under the European Community's Seventh Framework Programme (FP7/2007–2013), ERC grant agreement (205150), and the US National Science Foundation (EF 1040965).

Acknowledgements

We thank Ulrike Richter, Klaus-Uwe Richter, and Jana Hölscher for technical assistance at AWI, Gert-Jan Reichart and Mirja Hoins for $\delta^{13}C$-DIC measurements at Utrecht University, and Dieter Wolf-Gladrow as well as François M. M. Morel for constructive comments on the manuscript.

References

Badger MR, Andrews TJ, Whitney SM, Ludwig M, Yellowlees DC. 1998. The diversity and co-evolution of Rubisco, plastids, pyrenoids and chloroplast-based CO_2-concentrating mechanisms in algae. *Canadian Journal of Botany* **76,** 1052–1071.

Badger MR, Bassett M, Comins HN. 1985. A model for HCO_3^- accumulation and photosynthesis in the cyanobacterium *Synechococcus sp*. Theoretical predictions and experimental observations. *Plant Physiology* **77,** 465–471.

Badger MR, Palmqvist K, Yu JW. 1994. Measurement of CO_2 and HCO_3^- fluxes in cyanobacteria and microalgae during steady-state photosynthesis. *Physiologia Plantarum* **90,** 529–536.

Badger MR, Price GD, Long BM, Woodger FJ. 2006. The environmental plasticity and ecological genomics of the cyanobacterial CO_2 concentrating mechanism. *Journal of Experimental Botany* **57,** 249–265.

Buick R. 1992. The antiquity of oxygenic photosynthesis: evidence from stromatolites in sulphate-deficient Archaean lakes. *Science* **255,** 74–77.

Burkhardt S, Riebesell U, Zondervan I. 1999. Effects of growth rate, CO_2 concentration, and cell size on the stable carbon isotope fractionation in marine phytoplankton. *Geochimica et Cosmochimica Acta* **63,** 3729–3741.

Caldeira K, Wickett ME. 2003. Anthropogenic carbon and ocean pH. *Nature* **425,** 365–365.

Chen Y-B, Zehr JP, Mellon M. 1996. Growth and nitrogen fixation of the diazotrophic filamentous nonheterocystous cyanobacterium *Trichodesmium* sp. IMS 101 in defined media: evidence for a circadian rhythm. *Journal of Phycology* **32,** 916–923.

Dou Z, Heinhorst S, Williams EB, Murin CD, Shively JM, Cannon GC. 2008. CO_2 fixation kinetics of *Halothiobacillus neapolitanus* mutant carboxysomes lacking carbonic anhydrase suggest the shell acts as a diffusional barrier for CO_2. *The Journal of Biological Chemistry* **283,** 10377–10384.

Eichner M, Kranz SA, Rost B. 2014. Combined effects of different CO_2 levels and N sources on the diazotrophic cyanobacterium *Trichodesmium*. *Physiologia Plantarum* **152,** 316–330.

Espie GS, Kimber MS. 2011. Carboxysomes: cyanobacterial RubisCO comes in small packages. *Photosynthesis Research* **109,** 7–20.

Freeman KH, Hayes JM. 1992. Fractionation of carbon isotopes by phytoplankton and estimates of ancient CO_2 levels. *Global Biogeochemical Cycles* **6,** 185–198.

Guy RD, Fogel ML, Berry JA. 1993. Photosynthetic fractionation of stable isotopes of oxygen and carbon. *Plant Physiology* **101,** 37–47.

Holm-Hansen O, Riemann B. 1978. Chlorophyll a determination: improvements in methodology. *Oikos* **30,** 438–447.

Hopkinson BM, Dupont CL, Allen AE, Morel FMM. 2011. Efficiency of the CO_2-concentrating mechanism of diatoms. *Proceedings of the National Academy of Sciences, USA* **108,** 3830–3837.

Hutchins DA, Fu F-X, Zhang Y, Warner ME, Feng Y, Portune K, Bernhardt PW, Mulholland MR. 2007. CO_2 control of *Trichodesmium* N_2 fixation, photosynthesis, growth rates and elemental ratios: Implications for past, present and future ocean biogeochemistry. *Limnology and Oceanography* **552,** 1293–1304.

IPCC. 2007. Summary for policymakers. In: Solomon S, Qin D, Manning M, Chen Z, Marquis M, Averyt KB, Tignor M, Miller HL, eds. *Climate change 2007: the physical science basis. Contribution of working group I to the fourth assessment report of the Intergovernmental Panel on Climate Change*. Cambridge and New York: Cambridge University Press.

Kaplan A, Badger MR, Berry JA. 1980. Photosynthesis and the intracellular inorganic carbon pool in the bluegreen alga *Anabaena variabilis* - response to external CO_2 concentration. *Planta* **149,** 219–226.

Kasting JF, Siefert JL. 2002. Life and the evolution of earth's atmosphere. *Science* **296,** 1066–1068.

Keller K, Morel FMM. 1999. A model of carbon isotopic fractionation and active carbon uptake in phytoplankton. *Marine Ecology Progress Series* **182,** 295–298.

Klein MG, Zwart P, Bagby SC, Cai F, Chisholm SW, Heinhorst S, Cannon GC, Kerfeld CA. 2009. Identification and structural analysis of a novel carboxysome shell protein with implications for metabolite transport. *Journal of Molecular Biology* **392,** 319–333.

Kranz SA, Levitan O, Richter K-U, Prasil O, Berman-Frank I, Rost B. 2010. Combined effects of CO_2 and light on the N_2 fixing cyanobacterium *Trichodesmium* IMS101: Physiological responses. *Plant Physiology* **154,** 334–345.

Kranz SA, Sültemeyer D, Richter K-U, Rost B. 2009. Carbon acquisition in *Trichodesmium*: the effect of pCO_2 and diurnal changes. *Limnology and Oceanography* **54,** 548–559.

Laws EA, Bidigare RR, Popp BN. 1997. Effect of growth rate and CO_2 concentration on carbon isotopic fractionation by the marine diatom *Phaeodactylum tricornutum*. *Limnology and Oceanography* **42,** 1552–1560.

Levitan O, Rosenberg G, Setlik I, Setlikova E, Grigel J, Klepetar J, Prasil O., Berman-Frank I. (2007) Elevated CO_2 enhances nitrogen fixation and growth in the marine cyanobacterium *Trichodesmium*. *Global Change Biology* **13,** 531–538.

Maeda S, Badger MR, Price GD. 2002. Novel gene products associated with NdhD3/D4-containing NDH-1 complexes are involved in photosynthetic CO_2 hydration in the cyanobacterium *Synechococcus* sp. PCC7942. *Molecular Microbiology* **43,** 425–435.

Marcus Y, Schwarz R, Friedberg D, Kaplan A. 1986. High CO_2 requiring mutant of *Anacystis nidulans* R2. *Plant Physiology* **82,** 610–612.

Marlier JF, O'Leary MH. 1984. Carbon kinetic isotope effects on the hydration of carbon dioxide and the dehydration of bicarbonate ion. *Journal of the American Chemical Society* **106,** 5054–5057.

Mook W, Bommerson J, Staverman W. 1974. Carbon isotope fractionation between dissolved bicarbonate and gaseous carbon dioxide. *Earth and Planetary Science Letters* **22,** 169–176.

O'Leary M, Madhavan S, Paneth P. 1992. Physical and chemical basis of carbon isotope fractionation in plants. *Plant, Cell and Environment* **15,** 1099–1104.

Paneth P, O'Leary MH. 1985. Carbon isotope effect on dehydration of bicarbonate ion catalyzed by carbonic anhydrase. *Biochemistry* **24,** 5143–5147.

Price GD, Badger MR. 1989a. Ethoxyzolamide inhibition of CO_2 uptake in the cyanobacterium *Synechococcus* PCC7942 without apparent inhibition of internal carbonic anhydrase activity. *Plant Physiology* **89,** 37–43.

Price GD, Badger MR. 1989b. Ethoxyzolamide inhibition of CO_2-dependent photosynthesis in the cyanobacterium *Synechococcus* PCC7942. *Plant Physiology* **89,** 44–50.

Price GD, Badger MR. 1989c. Expression of human carbonic anhydrase in the cyanobacterium *Synechococcus* PCC7942 creates a high CO_2-requiring phenotype. Evidence for a central role for carboxysomes in the CO_2 concentrating mechanism. *Plant Physiology* **91,** 505–513.

Price GD, Badger MR, Woodger FJ, Long BM. 2008. Advances in understanding the cyanobacterial CO_2-concentrating-mechanism (CCM): functional components, C_i transporters, diversity, genetic regulation and prospects for engineering into plants. *Journal of Experimental Botany* **59,** 1441–1461.

Price GD, Maeda S, Omata T, Badger MR. 2002. Modes of inorganic carbon uptake in the cyanobacterium *Synechococcus* sp. PCC7942. *Functional Plant Biology* **29,** 131–149.

Reinhold L, Zviman M, Kaplan A. 1989. A quantitative model for inorganic carbon fluxes and photosynthesis in cyanobacteria. *Plant Physiology and Biochemistry* **27,** 945–954.

Roeske C, O'Leary M. 1984. Carbon isotope effects on the enzyme-catalyzed carboxilation of ribulose bisphosphate. *Biochemistry* **23,** 6275–6285.

Rost B, Kranz SA, Richter KU, Tortell PD. 2007. Isotope disequilibrium and mass spectrometric studies of inorganic carbon acquisition by phytoplankton. *Limnology and Oceanography: Methods* **5,** 328–337.

Rost B, Richter K-U, Riebesell U, Hansen PJ. 2006. Inorganic carbon acquisition in red tide dinoflagellates. *Plant, Cell and Environment* **29,** 810–822.

Rost B, Zondervan I, Wolf-Gladrow D. 2008. Sensitivity of phytoplankton to future changes in ocean carbonate chemistry: current knowledge, contradictions and research directions. *Marine Ecology Progress Series* **373,** 227–237.

Schulz KG, Rost B, Burkhardt S, Riebesell U, Thoms S, Wolf-Gladrow DA. 2007. The effect of iron availability on the regulation of inorganic carbon acquisition in the coccolithophore *Emiliania huxleyi* and the significance of cellular compartmentation for stable carbon isotope fractionation. *Geochimica et Cosmochimica Acta* **71,** 5301–5312.

Sharkey TD, Berry JA. 1985. Carbon isotope fractionation of algae influenced by an inducible CO_2-concentrating mechanism. In: Lucas WJ, Berry JA, eds. *Inorganic carbon uptake by aquatic photosynthetic organisms*. Rockville: American Society of Plant Physiologists, 389–401.

Tortell PD. 2000. Evolutionary and ecological perspectives on carbon acquisition in phytoplankton. *Limnology and Oceanography* **45,** 744–750.

Tchernov D, Lipschultz F. 2008. Carbon isotopic composition of *Trichodesmium* spp. colonies off Bermuda: effects of colony mass and season. *Journal of Plankton Research* **30,** 21–31.

Tsai Y, Sawaya MR, Cannon GC, Cai F, Williams EB, Heinhorst S, Kerfeld CA, Yeates TO. 2007. Structural analysis of CsoS1A and the protein shell of the *Halothiobacillus neapolitanus* carboxysome. *PLoS Biology* **5** doi: 10.1371/journal.pbio.0050144.

Williams PJL, Robertson JE. 1991. Overall planktonic oxygen and carbon dioxide metabolisms: the problem of reconciling observations and calculations of photosynthetic quotients. *Journal of Plankton Research* **13,** 153–169.

Zeebe RE, Wolf-Gladrow DA. 2007. *CO_2 in seawater: equilibrium, kinetics, isotopes*. Amsterdam: Elsevier Science B.V.